Intergranular Corrosion Evaluation of Heat Affected Zone of Ferritic Stainless Steel

Luciana Iglésias Lourenço Lima, lil@cdtn.br
Mônica Maria de Abreu Mendonça Schvartzman, monicas@cdtn.br
Marco Antônio Dutra Quinan, quinanm@cdtn.br
Wagner Reis da Costa Campos, wrcc@cdtn.br
Centro de Desenvolvimento da Tecnologia Nuclear (CDTN/CNEN-MG) - Rua Professor Mario Werneck s/n, 30123-970, Belo Horizonte, Minas Gerais

Alexandre Queiroz Bracarense, bracarense@ufmg.br
Estevão Zanata, zanata@gold.com.br
Universidade Federal de Minas Gerais (UFMG – MG) – Departamento de Engenharia Mecânica - Av. Antônio Carlos 6627, 31270-901, Belo Horizonte, Minas Gerais

Abstract. Stainless steels are a common construction material, as they offer a wide range of corrosion resistance, as well as good mechanical properties to many industrial environments (*e.g.*, chemical, fertilizer, petroleum, and nuclear industries). The stainless steel resistance occurs because of its ability to form a protective coating on the metal surface. This coating is a "passive" film which resists further to corrosion. The formation of this film is instantaneous in an oxidizing atmosphere such as air, water, or other fluids that contain oxygen. In the as welded condition, stainless steel can be susceptible to corrosion failures even though the proper base and filler metal have been selected, industrial and standards have been followed and that possess full weld penetration as well as proper shape have been deposited. Conventional 400-series ferritic stainless steels are susceptible to intergranular corrosion in the as-welded condition (sensitization). Corrosion in the weld area generally encompasses both the weld metal and the weld heat affected zone (HAZ). The objective of this work was to evaluate, by means of DL-EPR (double loop electrochemical potentiokinetic reactivation) and Pratice W (ASTM A763 standard), the degree of sensitization of an AISI 439 steel heat-affected zone (HAZ) submitted to two different weld heat inputs. The corrosion behavior of the samples was investigated by the potentiodynamic anodic polarization technique, which is used to determine the active/passive characteristics of a given metal-solution system. The robotic Gas Metal Arc Welding (GMAW) process using argon shielding gas and as filler metal an austenitic stainless steel AISI 308L-Si wire, was performed. The results were expressed by the relation Ir/Ia obtained by DL-EPR curve, for the two different weld heat inputs.

Keywords: AISI 439, intergranular corrosion, electrochemical potentiokinetic reactivation – double loop, heat affected zone, Pratice W.

1. INTRODUCTION

In the weld sector, corrosion is responsible for most of the problems that occur in service failures. This is because the weld regions are more susceptible to corrosion than the rest of the structure and the weld integrity can be dramatically reduced. Corrosion in the weld area generally encompasses both the weld metal and the weld heat affected zone (HAZ) (Fedele, 2005).

Stainless steels are used in chemical, nuclear and petroleum industries where corrosion resistance is an important factor. The stainless steel corrosion resistance is obtained with the presence of an oxide protector film on its surface and welding operations can affect the properties of this material. Conventional 400-series ferritic stainless steels are susceptible to intergranular corrosion in the as-welded condition (sensitization).

Sensitization is a term used to describe the depletion of chromium content brought about by the precipitation of chromium (Cr) rich carbides at the grain boundaries. The formation of the carbides requires the diffusion of chromium towards the grain boundaries, and this causes the formation a Cr depleted zone in the immediate vicinity of the boundary. The reduction of less than 10.5% weight percent of chromium content is harmful to the passive film formation and to the materials corrosion resistance (Serna-Giraldo, 2006).

The technique used to assess the susceptibility to intergranular corrosion can be immersion tests, as described, for example, in ASTM A262 standard for austenitic stainless steel and ASTM A763 standard for ferritic stainless steel. Practice W ASTM A763 standard shows the procedure to conduce metallographic etching with oxalic acid which is able to reveal phases rich in chromium. This practice is used for the acceptance of the material; however the materials rejection should be done through more accurate methods (Pires and Alonso-Falleiros, 2002).

During the last few years, the electrochemical techniques have been developed as an alternative to the use of immersion tests to assess the intergranular corrosion susceptibility of stainless steel and nickel based alloys. The method called electrochemical potentiokinetic reactivation has three versions: single loop (SL), double loop (DL) and the simplify (S). The advantages of these methods in correlation with immersion tests are mainly the lower execution time, higher accuracy and economy (Sedricks, 1996).

To assess the stainless steel weld corrosion resistance by electrochemical techniques it is necessary to do the separation of the weld zones (base metal, heat affected zone and weld metal) because their differences in chemical composition and microstructure can cause an electrochemical potential between the zones and lead to the attack by galvanic corrosion (Hemmingsen, et. al, 2002).

The objective of this work was to evaluate the degree of sensitization of an AISI 439 steel heat-affected zone (HAZ) submitted to two different heat inputs by means of the DL-EPR (double loop electrochemical potentiokinetic reactivation) technique and the Practice W of ASTM A763 standard.

2. EXPERIMENTAL PROCEDURES

The material used was the ferritic stainless steel AISI 439 whose composition are shown in Tab. 1.

Table 1. Composition of type AISI 439 (Acesita, 2004).

Chemical Composition (weight percent)									
C	Mn	P	S	Si	Ni	Cr	Mo	Al	Ti
0.0095	0.1434	0.0234	0.0027	0.4032	0.1777	17.1283	0.0191	0.0115	0.1984

The samples were obtained from a ferritic stainless steel AISI 439 weld plate. The dimensions of the weldment were 300 mm x 100 mm x 1.5 mm. The electrode used to weld, AISI 308L-Si, had a 1.2 mm and its composition is shown in Tab. 2.

Table 2. Composition of electrode AISI 308 L Si (Sandivick).

Chemical Composition (weight percent)						
C	Mn	P max.	S max.	Si	Ni	Cr
≤ 0.025	1.8	0.025	0.015	0.9	10.5	20

Welds using Motoman robotic GMAW formed under pure argon were 150 mm long. The welding conditions are summarized in Tab. 3.

Table 3. Welding Parameters.

Sample	Current (A)	Speed (mm/s)	Potential (V)	Stick Out (mm)	Heat Input (kJ)
1	105	8.33	20	25	252.1
2	57	8.33	13	25	88.9

Figure 1 shows the weldment.

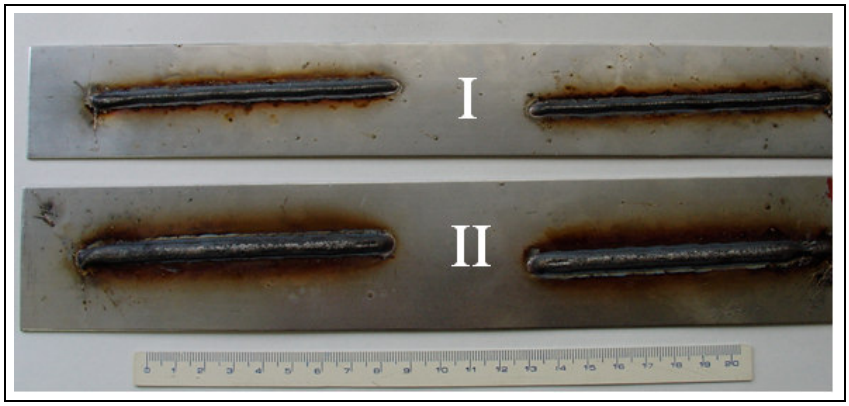

Figure 1. Sample welded, I – higher heat input and II – lower heat input.

The samples were cut in the weld transverse direction orientation and wet-polished until diamond solution 1µm was riched. The polished transversal section was attacked by Villela's reagent to reveal the microstructure.

In order to do the electrochemical tests, the HAZ was separated from the others regions. To determine the HAZ a photographic profile was made from the line fusion to the base metal, showed in Fig. 2.

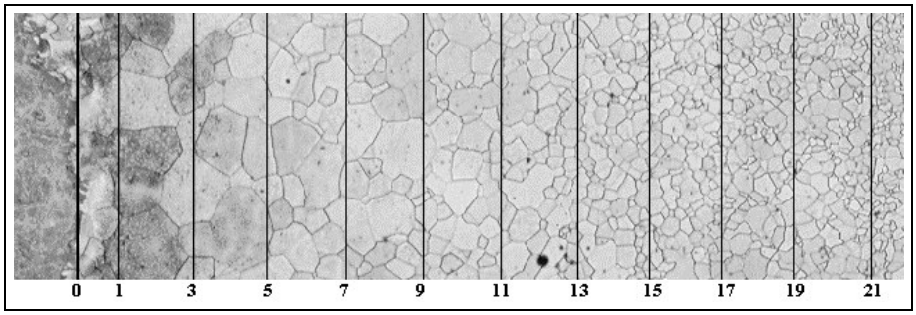

Figure 2. Heat affected zone photographic profile.

Parallel straight lines, all of the same length, were superimposed on the HAZ photomicrographic. The HAZ grain size fluctuation was determined by Heyn's method. This method consists in to count the number of intersections between the grains boundary and the each line segment, and then we divided the true line length by the number of intersections. For each line was determined the grain size and the each parallel straight line represent a distance from the fusion line, so we can get a profile grain size versus distance of the parallel straight line from fusion line (Lima, 2007).

The HAZ size was the region between the line fusion and the metal base which the average grain size was bigger or equal than 1/3 of the metal base average grain size. The metal base average grain size was measured by the software Quantikov which used the Saltykov's method (Pinto, 1996).

Standard ASTM A763 Practice W consists in an oxalic acid etch test used for acceptance of material but not rejection of material. This may be used in connection with other evaluation tests to provide a method for identifying the sensitization degree. The samples were prepared by epoxy cold resin and surfaces exposed to the electrolyte were prepared by sequential grinding and wet-polished up to diamond paste 1µm. The solution used for etching is prepared by adding 100 g of reagent grade acid oxalic to 900 ml of distilled water. The polished specimen should be etched at $1A/cm^2$ for 90 seconds.

The corrosion behavior of the samples was investigated by potentiodynamic anodic polarization and by *double loop electrochemical potentiokinetic reactivation* techniques. To study the corrosion behaviors of the materials, the tests were carried out with Autolab PGSTAT 20 potentiostat with GPES 4.4 software., The samples were tested under identical conditions for comparison. The samples were prepared by epoxy cold resin and surfaces exposed to the electrolyte were prepared by sequential grinding with silicon carbide paper up to 600 mesh finishing. Figure 3 shows the configuration of the samples used in electrochemical tests.

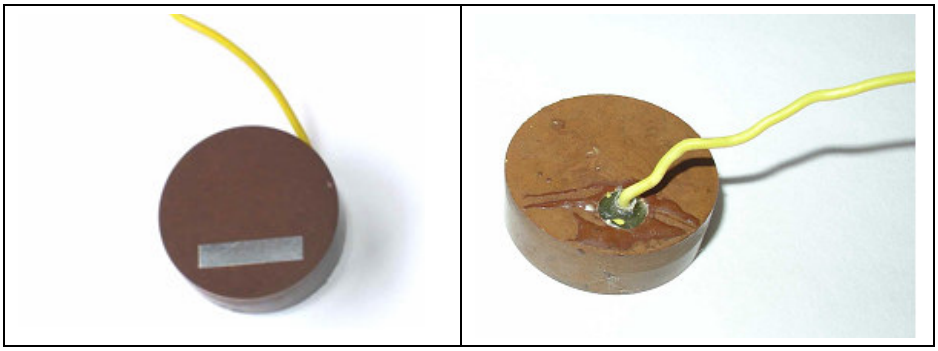

Figure 3. Samples used to electrochemical test.

A three-electrode cell arrangement was used for the electrochemical measurements, with a platinum wire and a Ag/AgCl electrode as the counter and reference electrodes, respectively. Electrochemical tests were performed at 30±1 ºC temperature in a de-aerated solution of 0.5N H_2SO_4. The tests were carried out in triplicate for each condition.

Potentiodynamic anodic polarization measurements were carried out at scan rate of 0.167 mV/s in the potential range - 200 mV from the open circuit potential (E_{ocp}), recorded after 50 minutes immersed (ASTM G5-94), up to 2,000 mV. The double loop test procedure was performed immersing the specimen in the solution at the open circuit potential for 5 minutes, polarizing the specimen from the open circuit potential to a potential in the passive region, +500 mV, and then back to the initial potential. The reverse polarization from the passive to the active region should give rise to a reactivation peak, the magnitude of which should be sensitive to the degree of alloy element depletion. The

susceptibility to corrosion is characterized in terms of either the ratio of the reactivation current peak to the activation current peak or the ratio of the reactivation charge to the activation charge.

3. RESULTS AND DISCUSSION

3.1. Metallographic characterization

The metal base microstructure (Fig. 4) has an equiaxial ferrite grain with some carbides and the average grain size is 21.3 μm. Table 4 shows the average grain size results table obtained by Quantikov software analyzer.

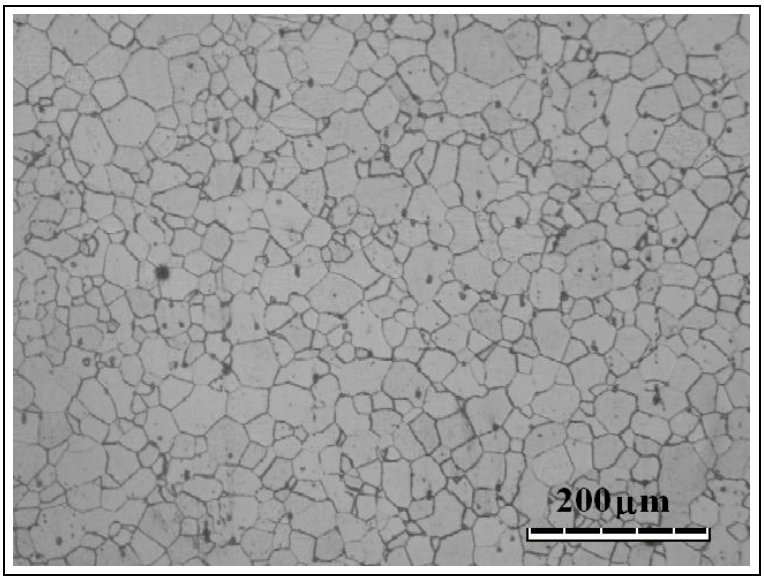

Figure 4. Base metal microstructure.

Table 4. Quantikov table results.

PROCESSING TABLE RESULTS
Quantikov Microstructural Analyzer 1/11/2006

Plain Distribution		
Type	**Diameter**	**Frequency**
1	60.000	0
2	58.167	0
3	56.333	3
4	54.500	2
5	52.667	1
6	50.833	0
7	49.000	2
8	47.167	7
9	45.333	3
10	43.500	8
11	41.667	7
12	39.833	13
13	38.000	13
14	36.167	14
15	34.333	18
16	32.500	27
17	30.667	19
18	28.833	30
19	27.000	25
20	25.167	35
21	23.333	36
22	21.500	38
23	19.667	37
24	17.833	41
25	16.000	41
26	14.167	31
27	12.333	39
28	10.500	49
29	8.667	24
30	6.833	32

Geometric Parameter	
Geometric Parameter	**(Micrometer)**
Average Width	26.6113
Width Standard Deviation	13.2396
Average Area	442.8933
Area Standard Deviation	424.583
Average Perimeter	94.7086
Perimeter Standard Deviation	49.8499
Major Area	2418.7667
Minor Area	20.1511
Average Diameter	21.2614
Diameter Standard Deviation	10.5853
Processed Elements	595
Processed Area/ Total Area	53.45

Stereometric Parameters	
Saltykov Method (three-dimensional distribution)	
Geometric Parameter	**(Micrometer)**
Sv Relation	0.0932
Average Intercept	21.4609
Sauter Diameter	31.6548

The Figure 5 shows the HAZ microstructure for the two heat inputs studied. It was observed a growth in the grain size with the increase of the heat input.

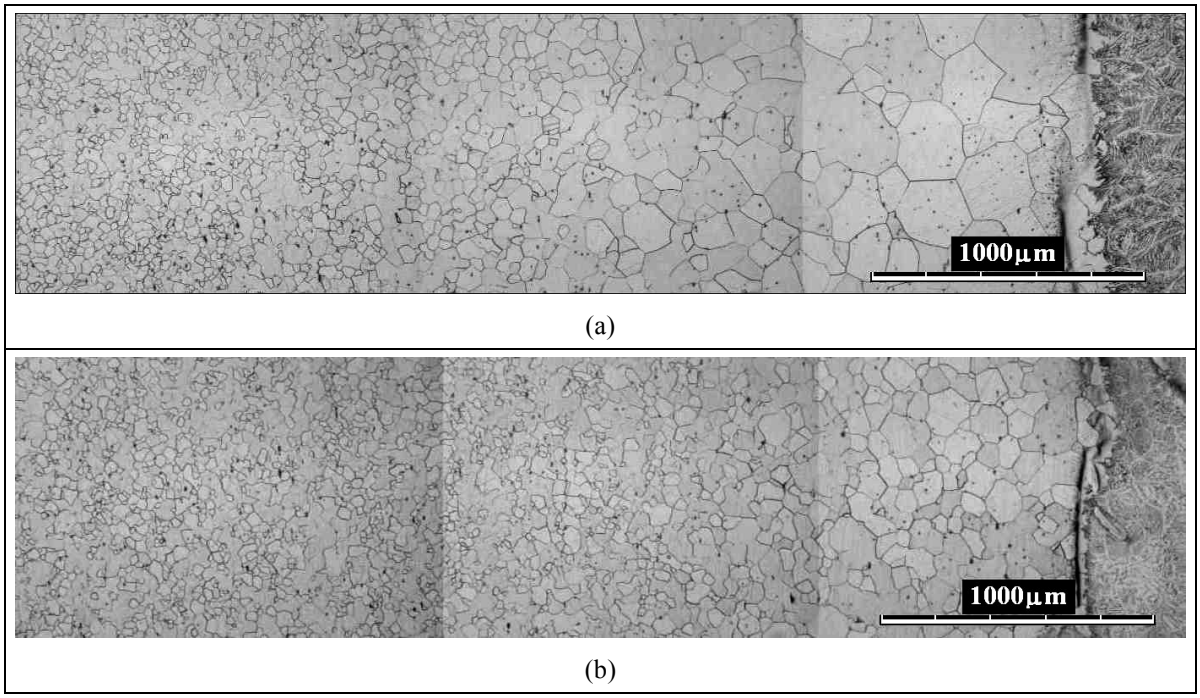

Figure 5. HAZ micrographic for the two heat inputs studied (a) higher heat input and (b) lower heat input.

3.2 Determination of the HAZ grain size

The HAZ average grain size, for each parallel line, was measured by Eq. 1:

$$Y = \frac{a}{b} \times 1000(\mu m) \tag{1}$$

Where:
Y = average grain size;
a = line length;
b = number of intersection.

The (average) HAZ grain size curves versus distance from the fusion line show an exponential behavior and can be represented using the Eq.2:

$$Y = Y_0 + A.e^{R_0.X} \tag{2}$$

Where:
Y = average grain size;
Y_0 = metal base average grain size;
X = distance between the straight lines and fusion line;
A and R_0 = equation parameters.

Figure 6 and 7 show the chart grain size versus distance from the fusion line for each sample. The HAZ size was determined used the criteria showed in the item 2. For the lower heat input sample the HAZ size was from the fusion line to 2 mm in direction to the base metal, and for the higher heat input sample this size was 4 mm.

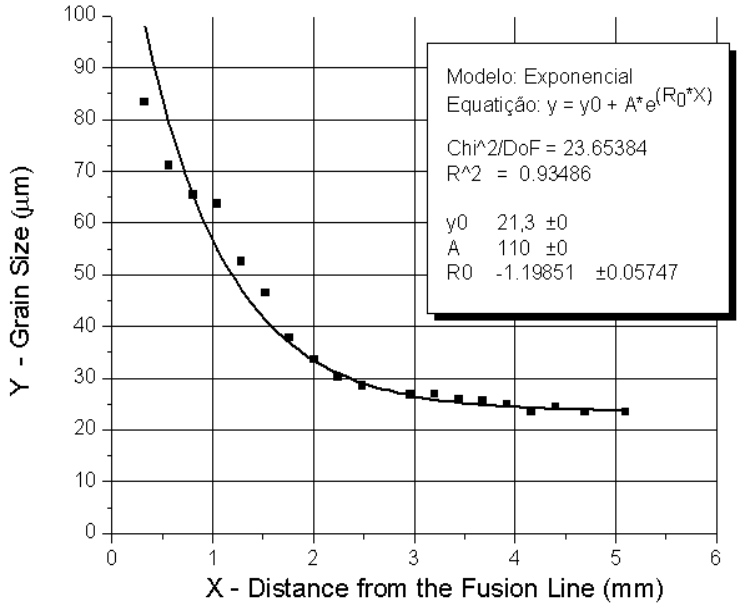

Figure 6. Curves grain size versus distance from the fusion line – sample lower heat input.

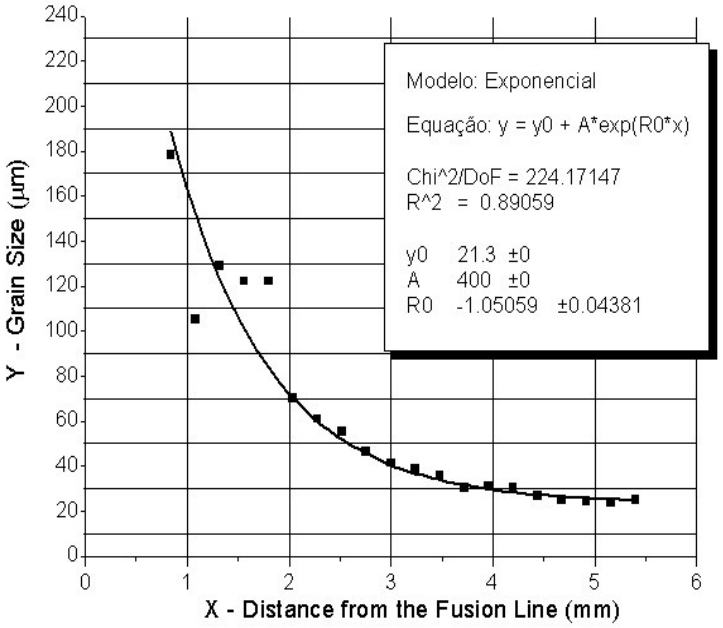

Figure 7. Curves grain size versus distance from the fusion line – sample higher heat input.

3.3. Pratice W – Standard ASTM A763

The micrographics for the metal base sample after the attacked was shown in Figure 8.

Ferrite grains and carbides in the matrix were observed. In the figure we can observe the mixed structure with ditches and steps. The step structure describes the absence of precipitates in the grain boundaries and the ditch structure means the presence of the phase rich in chromium. In this case, was observed the higher presence of step structure.

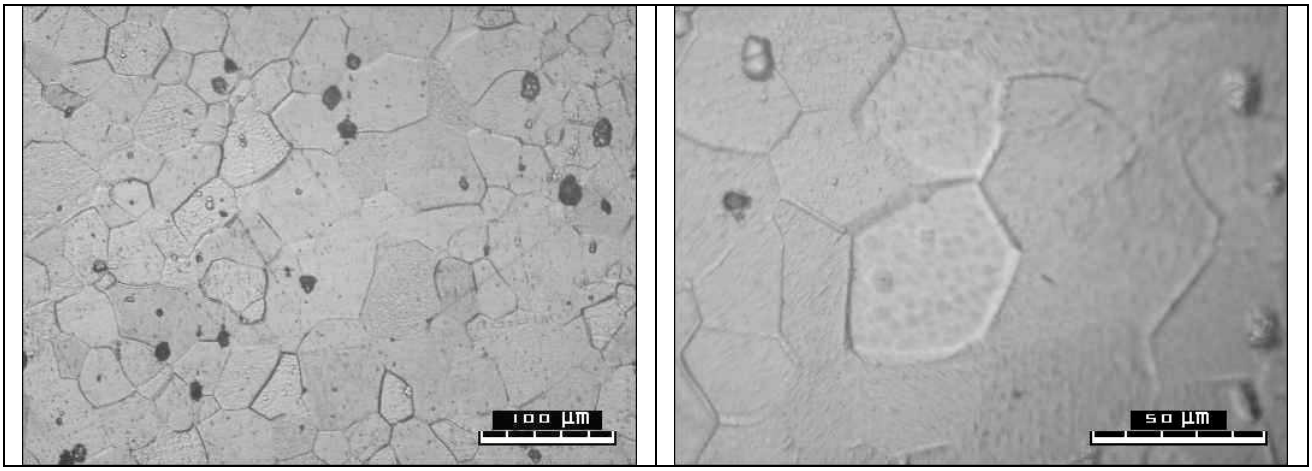

Figure 8 – Metal Base micrographic – Practice W.

Figure 9 shows the micrographics for the lower and higher input samples. The ditches cover all grain boundaries, which mean a higher sensitization degree.

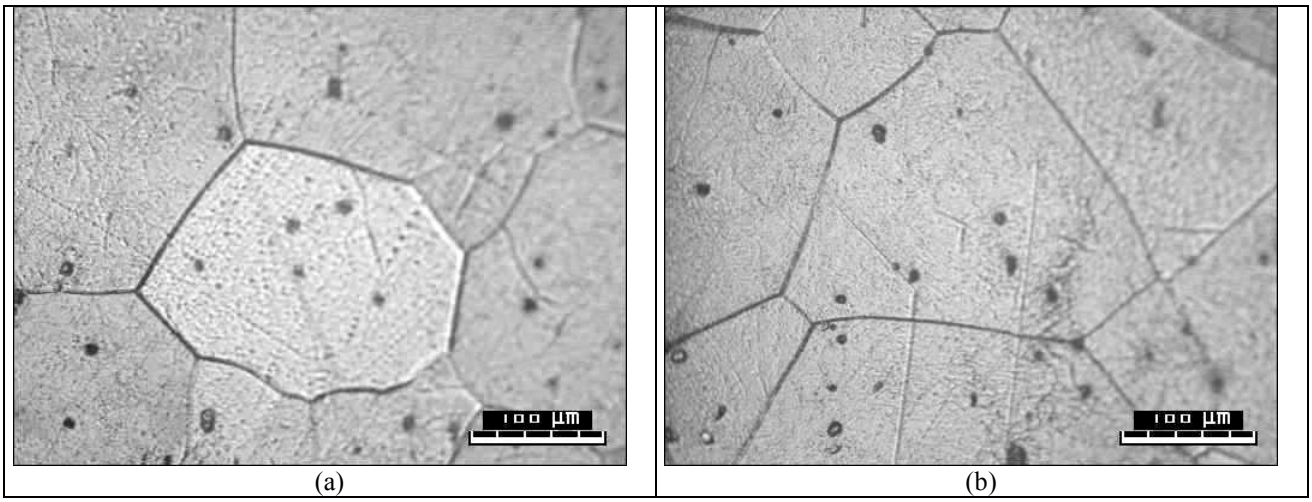

(a) (b)

Figure 9 – Slower (a) and higher (b) heat input micrographic – Practice W

All micrographics showed a structure ferritic and for the metal base sample was observed the formation of more step structure. For the slower and the higher heat input was observed the presence of the ditches, the precipitates cover all grain boundary. The electrolytic attacked in acid oxalic dissolved the rich chromium phases and the Fe-Cr-C-N system allowed the chromium carbides and nitrides precipitation. The cause of the ditches formation in the grain boundary is the carbides/nitrides dissolution (Cowan II and Tedmon, 1973).

3.4. Electrochemical tests

Figure 8 shows the anodic polarization curves for the three samples studied.

The three polarization curves show all similar behavior. Each curve has an "active-to-passive transition" and at more anodic potentials a transpassive region. The critic anodic current and the primary passivation potential were approximately in the same order. The current density in the passivation region whereas showed different values. This indicated different passivation degrees. For the metal base sample the current density was of the order 10^{-6} A/cm², for the lower heat input was of the order 10^{-5} A/cm². The higher heat input showed a variation from 10^{-5} A/cm² to 10^{-4} A/cm² in the current density. This variation observed in the passive region could be attributed to de chromium depletion in the regions adjacent to the grain boundary.

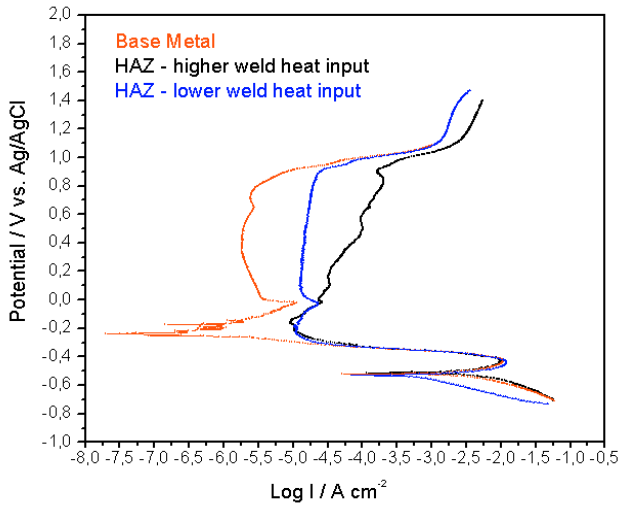

Figure 8. Anodic potentiodynamic polarization measurements.

The degree of sensitization (DOS) was determined by the ratio of the peak current observed when reactivating the grain boundaries (Ir) to the peak current observed when the entire surface was active (Ia), as shown in Figure 9.

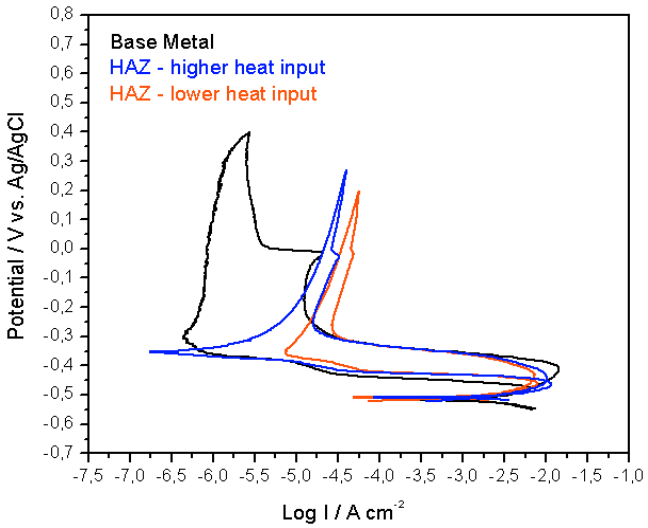

Figure 9. Double loop electrochemical potentiokinetic reactivation measurements.

The three potentiokinetic curves show in activation current densities in the same order of value and in reactivation the values were different. The curves that showed the higher Ir values demonstrated too the higher currents densities in the passive region.

It is important to notice that when the steel has a significant sensitization degree, the current densities in the second maximum anodic current and in the reactivation are higher than the lower or absence of sensitization. Table 5 shows the ratio Ir/Ia for the samples.

Table 5. Ratio Ir/Ia – sensitization degree.

Sample	Ir	Ia	Ir/Ia
Metal base	6.33×10^{-3}	1.43×10^{-2}	0.44
HAZ – higher heat input	1.15×10^{-2}	1.01×10^{-2}	1.14
HAZ – lower heat input	7.88×10^{-3}	7.29×10^{-3}	1.08

4. CONCLUSION

Immersion tests used in the present study were able to distinguish between sensitized and non-sensitized materials. However, the immersion tests were not able to distinguish subtle differences in the level of sensitization.

The DL-EPR test has been shown to be able to quantify small changes in the level of sensitization. There was, however, good agreement between the results obtained from immersion testing and DL-EPR testing.

5. ACKNOWLEDGEMENTS

The authors wish to express their appreciation to Capes, to Acesita for the material, to CNEN/CDTN and Laboratório de Robótica e Simulação for the laboratory support.

6. REFERENCES

Acesita - Aços Especiais Itabira - Grupo Arcelor, 2004, http://www.acesita.com.br/port/aco_inox/bib_catalogos.asp. Acessado em 20 out. 2005.

ASTM G5 - American Society for Testing and Materials - Standard Reference Test Method for Making Potentiostatic and Potentiodynamic Anodic Poalrization Measurements, 1994.

ASTM A763 - American Society for Testing and Materials - Standard Pratices for Detecting Susceptibility to Intergranular Attack in Ferritic Stainless, 1999.

Catálogo de produtos Sandivick.

Cowan II, R. L.; Tedmon, C.S. Intergranular corrosion of Iron-Nickel-Chromium alloys. In: Fontana, M. G.; Staehle, R. W. Advances in corrosion Science and Techonolgy, V.3, 1973.

Fedele, R.A. Corrosão intergranular em juntas soldadas, parte I, II, III. In: Revista Soldagem Inspeção Ano 6 nº 3. Disponível em: http://www.btwr.com.br **.** Acesso em: setembro, 2005.

Hemmingsen, T, Hovdan, H, Sanni, P, Aagotne, N.O. The influence of electrolyte potential on weld corrosion. Electrochimica Acta, 2002. V.47, p.3949-3952.

Lima, L. L. I., 2007, "Metodologia para Avaliação da Corrosão da Zona Termicamente Afetada de Aço Inoxidável Ferrítico AISI 439 Soldado", Dissertação de mestrado, Escola de Engenharia Mecânica - UFMG.

Pinto, L. C. M., 1996, Quantikov – Um analisador Microestrutural para um ambiente WindowsTM. Tese de Doutorado. Universidade de São Paulo/ Instituto de Pesquisas Energéticas e Nucleares – USP/IPEN.

Pires, R. F.; Alonso-Falleiros, N., 2002, Corrosão intergranular de aço inoxidável ferrítico: Avaliação através de método eletroquímico. Produção em Iniciação Científica da EPUSP. http://www.poli.usp.br. Acessado em 25 out 2005.

Sedricks, A. J., 1996, Corrosion of Staniless Steel. Second Edition. Princeton, New Jersey.

Serna-Giraldo, C. A., 2006, Resistência à Corrosão Intergranular UNS S43000: avaliação por método de reativação eletroquímica, efeito de tratamento isotérmico e mecanismo de sensitização. Tese de Doutorado. Escola Politécnica da Universidade de São Paulo.

7. RESPONSIBILITY NOTICE

The authors are the only responsible for the printed material included in this paper.